

Translesion synthesis past platinum DNA adducts by human DNA polymerase μ

[†] This research was supported in part by National Institute of Health grants CA84442-01 and
CA84480-03

*Jody M. Havener, Stephanie A. Nick McElhinny, Ekaterina Bassett, Michele Gauger, Dale A. Ramsden,
and Stephen G. Chaney**

Department of Biochemistry and Biophysics, Lineberger Comprehensive Cancer Center, School of
Medicine, University of North Carolina, Chapel Hill 27599-7260

** Corresponding author*

Running Title: Elongation past Pt-DNA adducts by DNA polymerase μ

Abbreviations: DNA polymerase μ , pol μ ; cisplatin, CP; oxaliplatin, OX

Corresponding Author: Stephen_Chaney@med.unc.edu, Phone (919) 966-3286, Fax (919) 966-2852

Abstract

DNA polymerase μ (pol μ) is a member of the pol X family of DNA polymerases, and it shares a number of characteristics of both DNA polymerase β (pol β) and terminal deoxynucleotidyl transferase (TdT). Because pol β has been shown to perform translesion DNA synthesis past cisplatin (CP)- and oxaliplatin (OX)-GG adducts, we determined the ability of pol μ to bypass these lesions. Pol μ bypassed CP and OX adducts with an efficiency of 14-35% compared to chain elongation on undamaged DNA, which is second only to pol η in terms of bypass efficiency. The OX adduct was bypassed with similar efficiency to that of the CP adduct, in contrast to other DNA polymerases studied. Since pol μ has been shown to be more efficient on gapped DNA templates than on primed single-stranded DNA templates, we determined the ability of pol μ to bypass Pt-DNA adducts on both primed single-stranded and gapped templates. The bypass of Pt-DNA adducts by pol μ was highly error-prone on all templates, resulting in 2, 3, and 4 nt deletions. We postulate that bypass of Pt-DNA adducts by pol μ may involve looping out the Pt-GG adduct to allow chain elongation downstream of the adduct. This reaction appears to be facilitated by the presence of a downstream "acceptor" and a gap large enough to provide undamaged template DNA for elongation past the adduct, although gapped DNA is clearly not required for bypass.

Keywords: translesion synthesis, DNA polymerase μ , cisplatin, oxaliplatin, lesion bypass

Cisplatin (CP) is widely used for the treatment of many malignancies including testicular, ovarian, head and neck, bladder, esophageal, and small cell lung cancers, but one of the major problems with its usage is acquired and intrinsic tumor resistance (1). Oxaliplatin (OX) is a second generation platinum complex that has been recently approved for use in the United States. OX is effective with colorectal and ovarian cancers and has been shown to be active in CP-resistant tumors (2). Both CP and OX exert their cytotoxic effects by forming intrastrand crosslinks on DNA (3), but cellular responses to treatment with these drugs differ (4). We have been interested in characterizing the mechanism(s) that determine the differences in the efficacy and mutagenicity of these two platinum complexes.

The extent and specificity of platinum resistance for CP and OX have been shown to correlate with the ability of cells to elongate DNA chains that contain platinum adducts (5, 6). For example, cells that are resistant to CP but not to OX show an increased ability to elongate DNA chains containing CP adducts, but not those containing OX adducts (5). These data suggest that total translesion synthesis is increased in CP-resistant cell lines and that in those cell lines translesion synthesis is greater for CP adducts than for OX adducts (7, 8). It has also been reported that OX is significantly less mutagenic than CP (9). These data suggest that error-prone translesion synthesis may discriminate between CP and OX adducts.

We and others have shown that human pol β and η can readily bypass platinum adducts *in vitro* in a relatively error-prone manner (10-12). Pol ζ can also bypass platinum adducts *in vitro*, but to a lesser extent than pol β or η (13), and all three of these enzymes have been shown to discriminate between CP and OX adducts (11). Pol ι and κ do not perform translesion synthesis past platinum adducts *in vitro* (14, 15), and the ability of pol μ and λ to perform translesion synthesis past platinum adducts has not yet been characterized.

The purpose of this study was to characterize the ability of pol μ to bypass CP and OX adducts *in vitro*. Pol μ is a member of the X family of polymerases, which also includes the template independent terminal deoxynucleotidyl transferase (TdT), pol β , and the recently identified pol λ and σ

(16). While the biological function of pol μ has yet to be determined, it has been proposed that it may function in either the non-homologous end-joining pathway for repair of double strand breaks or in V(D)J recombination for generation of antibody diversity during immunoglobulin development (17, 18). For example, Zhang *et al.* (17) have shown that pol μ promotes microhomology searching and pairing, and Mahajan *et al.* (18) have shown that pol μ associates with end-joining factors in cell culture and participates in end-joining reactions for repair of double-strand breaks *in vitro*. Zhang *et al.* (17) also reported that pol μ is more prone to frameshift mutations than base substitutions, which is consistent with the results reported here.

Pol μ may also function in translesion synthesis past bulky adducts. It can effectively bypass a *cis-syn* TT dimer in an error-free manner, but a template TT (6-4) photoproduct completely blocks synthesis (19). Pol μ is able to bypass abasic sites as well as 8-oxoguanine, 1, N^6 -ethenoadenine, *N*-2-acetylaminoflourine (AAF), and (+)- and (-)-*trans-anti*-benzo[*a*]pyrene- N^2 -dG adduct lesions (19). This was postulated to occur via primer realignment resulting in a frameshift past the lesion and therefore a deletion mutation. In the work reported here, we present evidence that pol μ is readily able to bypass CP and OX adducts *in vitro* by a postulated frameshift mechanism, and that no consistent pattern of discrimination between the two adducts is observed.

Methods and Materials

Construction of Platinum Adduct-containing Templates. Primer-templates were constructed from synthetic oligonucleotides purchased from Operon Technologies. Cisplatin was obtained from Sigma; Pt-(dach)Cl₂ (the biotransformation product of oxaliplatin) was provided by Sanofi-Synthelabo. All platination reactions were carried out with 40 mM aquated derivatives of the platinum complexes obtained by overnight stirring in the dark at room temperature of a solution containing either cisplatin or Pt-(dach)Cl₂ and 1.98 equivalents of silver nitrate. Platination of a 12mer oligonucleotide containing a single GG sequence (TCTAGGCCTTCT for 44mers or CTCTGGTCTTTA for 54mers) was performed

in the dark for 2 h at 37°C with a 2:1 drug to oligonucleotide ratio. The oligonucleotides containing a single platinum adduct were separated from unplatinated and overplatinated impurities by electrophoresis on a 20% polyacrylamide gel. DNA was eluted from gel slices by heating at 50°C for 30 m after soaking 10 h at 4°C and desalted using MicroSpin G25 columns.

The templates used for primer extension and nucleotide incorporation reactions are shown in Figures 1, 7, and 8. Control 44mers and 54mers were synthesized by Operon Technologies. Site-specifically platinated 44mer and 54mer templates were constructed as described previously (13). For the 44mers (Figures 1 and 8), a 35mer was used as a scaffold for hybridization of the platinated 12mers with a 14mer (left end) and an 18mer (right end). For the 54mers (Figure 7), a 44mer was used as a scaffold for hybridization of the platinated 12mers with a 24mer (left end) and an 18mer (right end). Following hybridization, 12mers were ligated to the left and right ends with T4 DNA Ligase. Ligation was performed for at least 10 h at 16°C and full length 44mers and 54mers were isolated by electrophoresis on a 12% denaturing polyacrylamide gel. DNA was eluted from gel slices by heating at 50°C for 30 m after soaking 10 h at 4°C and desalted using MicroSpin G25 columns.

There were two different types of primers used in these experiments: the first (24mer) terminated immediately 3' to the adduct, such that the first base added would be across from the 3'G of the platinum adduct (Figures 1 and 7), and the second (25mer) terminated opposite the 3'G of the adduct, such that the first base added would be across from the 5' base of the platinum adduct (Figure 8). The 24 or 25mer primers were 5'-end-labeled using T4 polynucleotide kinase and [γ -³²P]ATP for 2.5 h at 37°C in the dark. DNA substrates were prepared by annealing undamaged or platinated 44mer or 54mer templates with ³²P-labeled primers alone or in combination with downstream oligonucleotides (referred to as acceptors) at a 1:2.5:5 molar ratio. Hybridization was achieved by heating the mixture of required oligonucleotides in an annealing buffer (50 mM Tris-HCl (pH 8.0), 10 mM NaCl) for 10 m at 70°C, followed by slow cooling to room temperature over a period of about 2.5 h. Annealing efficiencies were >95%, as evidenced by the different mobility of the ³²P-labeled primers before and after hybridization to

the template and acceptors on native 12% polyacrylamide gels (data not shown).

Primer Extension Assays. Human pol μ was purified as previously described (18). Primer extension assays were performed as described previously (13) using undamaged and platinum-damaged templates. 75 fmol of primer-template or primer-template-acceptor (expressed as primer termini) was incubated with 75 fmol pol μ at 37°C in 8 μ l reactions containing 500 μ M dNTPs in a protein buffer containing 25 mM Tris-HCl (pH 7.5), 100 mM NaCl, 100 μ M EDTA, 2 mM DTT, 50 μ g/ml BSA, 0.05% Triton X-100, and 1% glycerol. Pol μ was diluted in 25 mM Tris-HCl (pH 8.0), 250 mM KCl, 2 mM DTT, 50 μ g/ml BSA, and 0.05% Triton X-100 prior to addition to the reaction. Reaction times varied and are indicated in the figure legends. Reactions were terminated by adding 8 μ l of denaturing loading dye solution (500 mM EDTA, 0.1% xylene cyanol, and 0.1% bromophenol blue in 90% formamide) and immediately placing on ice. Before separation by electrophoresis, samples were denatured at 100°C for 10 m and immediately transferred to ice. Products were resolved by denaturing polyacrylamide gel electrophoresis (8 M urea, 16% acrylamide, 4 h at 2000 V) and then visualized and quantified using a Molecular Dynamics PhosphorImager and Image Quant software. The extent of primer elongation on undamaged templates was calculated as the sum of primer extension as a percent of total primer termini (elongated and unelongated). The extent of translesion synthesis was calculated as the sum of primer extension past the platinum adducts, including bases across from and downstream of the adduct, as a percent of total primer termini (elongated and unelongated).

Nucleotide Incorporation Assays. To measure nucleotide incorporation opposite Pt-GG adducts, the DNA substrates listed above were used. Reactions were performed as described in the previous section with the exception that 500 μ M of a single dNTP was added to each reaction. Reactions were terminated, and products were analyzed as described above.

Results

Primer Extension with a Primer Terminating Immediately Prior to the Adduct on CTAGGC Templates.

Recent studies have shown that gapped DNA is a better substrate for pol μ than primed single-stranded DNA (S.A. Nick McElhinny and D.A. Ramsden, manuscript submitted). Therefore, we initially compared both chain elongation on undamaged templates and bypass of CP and OX adducts on primed single-stranded templates and templates with a one, two, three, or four nucleotide gap. For the initial experiments we used a primer that terminated immediately prior to the adduct and 44mer templates that were either undamaged or contained a single platinum-GG adduct in the CTAGGGC sequence context (the underlined section indicates the position of the platinum adduct, when present) (Figure 1). Figure 2 shows the results of the primer extension assays on undamaged and platinum-damaged templates (not all time points are shown). These experiments demonstrate the ability of pol μ to bypass the platinum adducts, but they also suggest that pol μ has the ability to displace the acceptor strand, as the size of the gap influences but does not dictate the exact number of nucleotides inserted. The data obtained from at least three replicate experiments are summarized in Figures 3 and 4. With undamaged templates the efficiency of chain elongation was 1 nucleotide (nt) > primed single-stranded > 2 nt > 3 nt > 4 nt (Figure 3A). These data confirm previous observations that pol μ prefers gapped DNA to primed single-stranded DNA, but the efficiency of chain elongation quickly diminishes with increasing gap size, and larger gaps appear to actually interfere with chain elongation on undamaged templates.

With platinum-damaged templates the overall efficiency of chain elongation was greatest for the 3 nt gap template and similar for all other templates (Figure 3B). Figure 4 compares the extent of chain elongation on undamaged and platinated DNA templates with different gap sizes. It is important to note that the incubation times have been optimized for each template and gap size. Thus, incubation times vary for each template, but all of the experiments contain some times that overlap. Translesion synthesis is defined here as the sum of all primer extension past the adduct, including bases across from and downstream of the adduct, as a percent of total primer-termini (elongated and unelongated). The extent of translesion synthesis past platinum adducts as compared to chain elongation on undamaged DNA was interesting: translesion synthesis was 14-35% of synthesis on undamaged templates with primed single-

stranded templates, 2.5-10% of undamaged with a 1 nt gap, 10-30% of undamaged with a 2 nt gap, approximately equal to the undamaged with a 3 nt gap, and 1.5 to 2-fold greater than the undamaged with a 4 nt gap. The 1 and 2 nt gap clearly interfered with translesion synthesis, while the 3 and 4 nt gap greatly enhanced translesion synthesis. However, it should be emphasized that pol μ is relatively inefficient on undamaged 3 and 4 nt gap DNA templates (Figure 3A). Thus, only the 3 nt gap template offers an advantage over the primed single-stranded template in terms of translesion synthesis on platinated templates (Figure 3B). When comparing the effect of CP adducts to the effect of OX adducts on the extent of translesion synthesis, no simple pattern was evident.

Nucleotide Incorporation with a Primer Terminating Immediately Prior to the Adduct on CTAGGC Templates. In order to obtain a better understanding of the mechanism(s) leading to the observed patterns of translesion synthesis, we examined the pattern of dNTP incorporation with each of the CTAGGC templates (Figures 5 and 6). With this template sequence, a high frequency of dTTP incorporation suggests a 2 nt frameshift, dATP incorporation suggests a 3 nt frameshift, and dGTP incorporation suggests a 4 nt frameshift. When we looked at undamaged primed single-stranded DNA, some dTTP misincorporation was observed compared to correct dCTP incorporation (Figure 5), consistent with the hypothesis that a small amount of 2 nt frameshifts occurs even on undamaged DNA. The frequency of dTTP misincorporation on undamaged DNA was 3 nt > 2 nt > 1 nt > 4 nt \geq primed single-stranded (Figure 6A). In fact, with the undamaged 3 nt gap template the frequency of dTTP misincorporation was greater than correct dCTP incorporation. This suggests that the presence of a downstream acceptor on the 3 nt gap template significantly increases the probability of the 2 nt frameshift that enhances dTTP incorporation. The fact that substantial dTTP misincorporation was seen with the 1 and 2 nt gap templates was surprising because the template A was covered by the acceptor strand on those templates. This suggests that pol μ has the ability to catalyze strand displacement, which is consistent with the primer extension patterns seen in Figure 2.

The presence of a platinum adduct significantly facilitated dTTP, dATP, and dGTP

misincorporation on most templates (Figures 5 and 6). This suggests that the presence of a platinum adduct either greatly decreases the fidelity of pol μ or, more likely based on a previous report of highly frequent frameshifts (17), facilitates 2, 3, and even 4 nt frameshifts. The frequency of dATP misincorporation on platinum-damaged templates was 4 nt \cong 3 nt > 2 nt \cong 1 nt \cong primed single-stranded (Figure 6B). These data suggest that the presence of the downstream acceptor also facilitates the 3 nt frameshift that enhances dATP incorporation. Incorporation of dATP with the 3, 2, and 1 nt gap templates requires strand displacement of 1, 2, and 3 nt, respectively. Thus, these data suggest that a 1 nt strand displacement to uncover the template T is well tolerated, but requirement of a 2 or 3 nt strand displacement to uncover the templating base inhibits the ability of pol μ to frameshift. For dGTP misincorporation, the frequency on platinum-damaged templates was primed single-stranded > 1 nt \cong 2 nt \cong 3 nt \cong 4 nt (Figure 6C). This is most likely due to the fact that only on the primed single-stranded template is the template C not covered by an acceptor strand. The pattern of misincorporation was generally similar with CP and OX adducts for 1 and 4 nt gap templates, but with primed single-stranded templates OX adducts favored dGTP misincorporation and with 2 and 3 nt gap templates OX adducts favored dTTP misincorporation.

Primer Extension and Nucleotide Incorporation with a Primer Terminating Immediately Prior to the Adduct on TCTGGT Templates. The patterns of misincorporation described in the previous section could have been due to simple misincorporation opposite the templating DNA rather than a realignment of the primer on the template to result in a frameshift. Therefore we determined the frequencies and patterns of misincorporation with 3 and 4 nt gap templates in which the platinum-GG adduct was placed in the TCTGGT sequence context (Figure 7). If most of the dTTP misincorporation seen with the 3 nt gap in the previous sequence context were due to a 2 nt frameshift rather than simple misincorporation opposite the template 3'G, one would predict that dATP incorporation would become more frequent than dTTP incorporation with this template sequence. Pol μ has also been reported to be facile at searching for regions of downstream microhomology and realigning the primer to create larger gaps

(17). Thus, one might predict that dGTP misincorporation should increase with this template, particularly with the 4 nt gap where no strand displacement would be required for dGTP incorporation. As shown in Figure 7, the extent of translesion synthesis is significant with both the 3 and 4 nt gap, and the pattern of misincorporation is exactly what one would expect for a frameshift model of translesion synthesis. With the 3 nt gap dATP misincorporation becomes predominant, but dGTP misincorporation is also greater than dTTP misincorporation. With the 4 nt gap dGTP misincorporation becomes predominant, consistent with the hypothesis that the primer terminus would realign with a homologous base downstream. As before, the presence of the platinum adduct appeared to favor the tendency to frameshift.

Primer Extension and Nucleotide Incorporation with a Primer Terminating Across from the 3'G of the Adduct on CTAGGC Templates. Pol μ has also been reported to be particularly prone to frameshifts when the template DNA has base repeats (17). Thus, to better test the effect of the repeating GG sequence on the ability of pol μ to catalyze frameshifts, we returned to the original templates, but used a primer terminating in C opposite the 3'G of the platinum adduct, as shown in Figure 8. One would predict that this would greatly facilitate the bypass of platinum adducts because the primer terminus could realign one base downstream to the 5' base of the adduct, and would therefore increase the frequency of dTTP and possibly dATP misincorporation. Figures 9 and 10 shows the results of the primer extension assays on undamaged and platinum damaged templates. As shown in Figure 10, the extent of chain elongation on undamaged templates was 1 nt \cong 2 nt > 3 nt > primed single-stranded. The extent of translesion synthesis was significantly increased for all templates except for the 3 nt gap by this primer-template alignment. With the previous primer on this template, the maximum amount of translesion synthesis observed on templates except for the 3 nt gap was about 20-30%, whereas the same templates with this primer achieved 60-80% translesion synthesis. The pattern of nucleotide incorporation is shown in Figure 11. dTTP, dATP, and dGTP misincorporation was significantly increased for all four templates with a frequency of 3 nt > 2 nt > 1 nt \cong primed single-stranded. These

data are consistent with the hypothesis that base repeats at a site of primer terminus homology significantly increase the probability of both frameshifts and translesion synthesis.

Discussion

Previous studies have shown that pol η and β can bypass platinum adducts with high efficiency (11, 13), pol ζ with low efficiency (13), and pol ι and κ are unable to bypass platinum adducts (14, 15). The abilities of pol μ and pol λ to bypass platinum adducts had not been previously characterized, although pol μ has been shown to bypass AAF and other bulky adducts (20).

With several DNA polymerases it is possible to obtain extensive translesion synthesis simply by utilizing high enzyme to template ratios and long incubation times, although these conditions are not physiologically relevant. To accurately assess the relative ability of DNA polymerases to catalyze translesion synthesis it is necessary to perform the experiments under conditions in which the time-dependent elongation by each polymerase on the undamaged template is in the linear range (13). With pol μ , conditions of linearity with the primed single-stranded template were achieved during the first 15 min of incubation at 1:1 ratios of enzyme to template (Figure 4A). Under these conditions, pol μ catalyzed 14-35% translesion synthesis past platinum adducts as compared to chain elongation on undamaged DNA. At similar enzyme to template ratios and conditions of linearity, human pol η , human pol β , and yeast pol ζ catalyze 35-75% (11), 6-12% (13), and 5-9% translesion synthesis (13), respectively. Thus, pol μ is somewhat less efficient than pol η at catalyzing translesion synthesis past platinum adducts *in vitro*, but appears to be significantly more efficient than pol β or pol ζ . The *in vivo* significance of these data is unclear, but does suggest that pol μ could potentially play a role in translesion synthesis past platinum adducts *in vivo*.

The mechanism of translesion synthesis past platinum adducts by pol μ was clarified by determining the effect of template structure on both chain elongation with undamaged DNA templates

and translesion synthesis past platinum adducts. Previous studies have shown that gapped DNA was a better template for pol μ than primed single-stranded templates (S.A. Nick McElhinny and D.A. Ramsden, manuscript submitted), and this was confirmed with our results. Here we compare the effect of gap size on synthesis on undamaged templates versus translesion synthesis past a platinum adduct. With undamaged DNA the efficiency of chain elongation was 3-fold greater with a 1 nt gap than with primed single-stranded DNA. However, the efficiency of chain elongation decreased rapidly with increasing gap size (Figure 3). This is very similar to the template preferences observed with pol β (21). It suggests that pol μ has a binding site for the acceptor strand on the 5' side of a very short (1 nt) gap and that binding of the acceptor strand facilitates chain elongation. In the case of pol β , the 5' acceptor binds to an 8 kDa domain (21), and pol μ has a region of sequence homology to the 8 kDa domain of pol β (22).

When the effect of gap size on translesion synthesis was studied, a very interesting pattern was observed. Total chain elongation past platinum adducts was greater on templates with a 3 nt gap than on primed single-stranded templates (Figure 3B). Furthermore, translesion synthesis past platinum adducts was actually equal to chain elongation with undamaged DNA on templates with a 3 nt gap (Figure 4D) and was 1.5 to 2-fold greater than chain elongation on undamaged DNA on templates with a 4 nt gap (Figure 4E). Thus, while platinum adducts were a partial block to chain elongation on primed single-stranded templates and templates with 1 or 2 nt gaps, they did not inhibit chain elongation whatsoever on templates with 3 nt gaps and actually facilitated chain elongation on templates with 4 nt gaps. It should be noted that while total chain elongation was greatest on platinated templates with a 3 nt gap, it was still substantial on primed single-stranded templates (Figure 3B). Thus, while the gapped templates provided clues to the mechanism of translesion synthesis, the presence of a gap is clearly not required for translesion synthesis.

The nucleotide incorporation data on both undamaged and platinum adduct-containing DNA provided another clue to the mechanism of enhanced translesion synthesis on templates with 3 and 4 nt

gaps. When the pattern of nucleotide incorporation was evaluated opposite the first base of the platinum adduct on primed single-stranded undamaged DNA, there was a significant amount of dTTP misincorporation compared to correct dCTP incorporation (Figure 5A and 6A). This particularly high error frequency could have arisen by one of two mechanisms: either simple misincorporation opposite the platinum adduct or a 2 nt frameshift, which would require a looping out of the template DNA. dTTP misincorporation increased slightly with the 1 and 2 nt gap templates (Figure 6A), which is somewhat surprising considering that the template A was covered by the acceptor strand with both of these templates (Figure 1). However, with the 3 nt gap template, the templating A is not covered by the acceptor strand, and with this template dTTP misincorporation was greater than or equal to dCTP incorporation (Figure 6A). This dramatic increase in dTTP incorporation would be difficult to rationalize on the basis of simple misincorporation, but would be fully consistent with a 2 nt frameshift. We postulate that the downstream acceptor interacts with pol μ in such a way as to stabilize the looping out of the template strand that is necessary to facilitate a 2 nt frameshift. Interestingly, dTTP misincorporation decreased significantly with the 4 nt gap template. Presumably the acceptor strand was now positioned too far from the primer to facilitate the 2 nt frameshift.

Platinum adducts significantly increased dTTP, dATP, and dGTP misincorporation with all of the templates tested (Figures 5, 6, 7E-F, and 11), suggesting that the platinum adduct also destabilizes the DNA sufficiently to facilitate the looping out required to generate 2, 3, and 4 nt frameshifts. These data are consistent with NMR (23-25) and *in vitro* frameshift studies with pol β and pol η (26) which suggest that the presence of a platinum adduct can facilitate loop formation. These data also suggest that if pol μ does contribute to bypass of platinum adducts *in vivo*, it would primarily generate deletion mutations. Platinum drugs cause about 15-23% deletion mutations in eukaryotic cells *in vivo* (27-29). Thus, while pol μ may participate, it is unlikely to play the primary role in error-prone translesion synthesis past platinum adducts *in vivo*.

Zhang *et al.* (19) have shown that pol μ can efficiently bypass a number of bulky DNA lesions,

and they postulated that this occurs by a primer realignment which results in a deletion of the base(s) opposite the adduct. This is essentially the same mechanism that we have proposed for the bypass of platinum adducts by pol μ . It should be noted that most of the frameshifts observed by us and by Zhang *et al.* (19) do not involve the alignment of the primer end with a complementary base downstream of the adduct. Thus, we have chosen to describe this mechanism as a looping out of the template strand rather than a primer realignment. Duvauchelle *et al.* (20) have reported that, in the presence of proteins in human primary fibroblast extracts, pol μ repeatedly incorporates a single nucleotide at the end of a growing chain. They postulated that this was due to a slipped intermediate containing several looped out bases. In this study we observe the same type of single nucleotide chain elongation (Figure 5A) in the absence of any auxiliary factor(s). This chain elongation was particularly striking in the case of the 3 nt gap DNA with the OX adduct where a ladder of up to 13 dTMPs was observed (Figure 5D). The postulate of a slipped intermediate containing looped out bases (20) is very similar to the mechanism that we have proposed for the observed 2, 3, and 4 nt frameshifts. These data suggest that the ability to tolerate looped out bases in the template strand is an inherent property of pol μ . It can be enhanced by auxiliary factors (20), the presence of a downstream acceptor, a platinum adduct, or other bulky DNA lesions (19). The ability to tolerate looped out bases in the template strand can facilitate frameshifts or, in the case of a single dNTP substrate, repeated incorporation of that nucleotide into a growing chain. The ability of pol μ to tolerate looped out bases and frameshifts also appears to greatly enhance its ability to bypass platinum adducts.

In summary, our data show that pol μ bypasses platinum adducts *in vitro* with efficiency second only to that observed with pol η . These data suggest that pol μ could play a role in translesion synthesis past platinum-DNA adducts *in vivo*. While most other DNA polymerases studied differed significantly in their ability to bypass CP and OX adducts (13), pol μ showed no consistent ability to distinguish between the adducts formed by these platinum complexes. Our data also confirm previous reports that pol μ is substantially error-prone, catalyzing 2, 3, and 4 nt frameshifts with high frequency and, in some

sequence contexts, searching out downstream regions of microhomology before continuing chain elongation. These types of errors would likely require a looping out of the template strand. Our data suggest that the looping out of the template strand necessary to generate these frameshifts is facilitated by the presence of platinum adducts and/or gapped templates of suitable length. Thus, if pol μ does contribute to translesion synthesis past platinum adducts *in vivo*, it is likely to do so in a highly error-prone manner, perhaps contributing to the deletion mutations observed in platinum-treated eukaryotic cells.

Acknowledgements

We thank Dr. J. T. Reardon and Dr. A. Vaisman for critical reading and improvement of the manuscript. S.A. Nick McElhinny was supported by a National Science Foundation Graduate Research Fellowship.

References

1. Zamble, D. B., and Lippard, S. J. (1995) Cisplatin and DNA repair in cancer chemotherapy, *Trends Biochem. Sci.* 20, 435-439.
2. Chaney, S. G., and Vaisman, A. (1999) Specificity of platinum-DNA adduct repair, *J. Inorg. Biochem.* 77, 71-81.
3. Eastman, A. (1987) Glutathione-mediated activation of anticancer platinum(IV) complexes, *Biochem. Pharmacol.* 36, 4177-4178.
4. Schmidt, W., and Chaney, S. G. (1993) Role of carrier ligand in platinum resistance of human carcinoma cell lines, *Cancer Res.* 53, 799-805.
5. Mamenta, E. L., Poma, E. E., Kaufmann, W. K., Delmastro, D. A., Grady, H. L., and Chaney, S. G. (1994) Enhanced replicative bypass of platinum-DNA adducts in cisplatin-resistant human ovarian carcinoma cell lines, *Cancer Res.* 54, 3500-3505.
6. Fruhauf, S., and Zeller, W. J. (1991) New platinum, titanium, and ruthenium complexes with different patterns of DNA damage in rat ovarian tumor cells, *Cancer Res.* 51, 2943-2948.
7. Gibbons, G. R., Kaufmann, W. K., and Chaney, S. G. (1991) Role of DNA replication in carrier-ligand-specific resistance to platinum compounds in L1210 cells, *Carcinogenesis* 12, 2253-2257.
8. Vaisman, A., Varchenko, M., Umar, A., Kunkel, T. A., Risinger, J. I., Barrett, J. C., Hamilton, T. C., and Chaney, S. G. (1998) The role of hMLH1, hMSH3, and hMSH6 defects in cisplatin and oxaliplatin resistance: Correlation with replicative bypass of platinum-DNA adducts, *Cancer Res.* 58, 3579-3585.
9. Leopold, W. R., Batzinger, R. P., Miller, E. C., Miller, J. A., and Earhart, R. H. (1981) Mutagenicity, tumorigenicity, and electrophilic reactivity of the stereoisomeric platinum(II)

- complexes of 1,2-diaminocyclohexane, *Cancer Res.* *41*, 4368-4377.
10. Masutani, C., Kusumoto, R., Iwai, S., and Hanaoka, F. (2000) Mechanisms of accurate translesion synthesis by human DNA polymerase η , *EMBO J.* *19*, 3100-3109.
 11. Vaisman, A., Masutani, C., Hanaoka, F., and Chaney, S. G. (2000) Efficient translesion replication past oxaliplatin and cisplatin GpG adducts by human DNA polymerase η , *Biochemistry* *39*, 4575-4580.
 12. Yuan, F., Zhang, Y., Rajpal, D. K., Wu, X., Guo, D., Wang, M., Taylor, J. S., and Wang, Z. (2000) Specificity of lesion bypass by the yeast DNA polymerase η , *J. Biol. Chem.* *275*, 8233-8239.
 13. Vaisman, A., Lim, S. E., Patrick, S. M., Copeland, W. C., Hinkle, D. C., Turchi, J. J., and Chaney, S. G. (1999) Effect of DNA Polymerases and High Mobility Group Protein 1 on the Carrier Ligand Specificity for Translesion Synthesis past Platinum-DNA Adducts, *Biochemistry* *38*, 11026-11039.
 14. Johnson, R. E., Washington, M. T., Haracska, L., Prakash, S., and Prakash, L. (2000) Role of DNA polymerase η in the bypass of a (6-4) TT photoproduct, *Nature* *406*, 1015-1019.
 15. Ohashi, E., Ogi, T., Kusumoto, R., Iwai, S., Masutani, C., Hanaoka, F., and Ohmori, H. (2000) Error-prone bypass of certain DNA lesions by the human DNA polymerase κ , *Genes Dev.* *14*, 1589-1594.
 16. Burgers, P. M., Koonin, E. V., Bruford, E., Blanco, L., Burtis, K. C., Christman, M. F., Copeland, W. C., Friedberg, E. C., Hanaoka, F., Hinkle, D. C., Lawrence, C. W., Nakanishi, M., Ohmori, H., Prakash, L., Prakash, S., Reynaud, C. A., Sugino, A., Todo, T., Wang, Z., Weill, J. C., and Woodgate, R. (2001) Eukaryotic DNA polymerases: proposal for a revised

- nomenclature, *J. Biol. Chem.* 276, 43487-43490.
17. Zhang, Y., Wu, X., Yuan, F., Xie, Z., and Wang, Z. (2001) Highly frequent frameshift DNA synthesis by human DNA polymerase μ , *Mol. Cell Biol.* 21, 7995-8006.
 18. Mahajan, K. N., Nick McElhinny, S. A., Mitchell, B. S., and Ramsden, D. A. (2002) Association of DNA polymerase mu (pol μ) with Ku and ligase IV: role for pol mu in end-joining double-strand break repair, *Mol. Cell Biol.* 22, 5194-5202.
 19. Zhang, Y., Wu, X., Guo, D., Rechkoblit, O., Taylor, J.-S., Geacintov, N. E., and Wang, Z. (2002) Lesion bypass activities of human DNA polymerase μ , *J. Biol. Chem.*, *epub ahead of print*.
 20. Duvauchelle, J.-B., Blanco, L., Fuchs, R. P. P., and Cordonnier, A. M. (2002) Human DNA polymerase mu (Pol μ) exhibits an unusual replication slippage ability at AAF lesion, *Nucl. Acids Res.* 30, 2061-2067.
 21. Rajendran, S., Jezewska, M. J., and Bujalowski, W. (2001) Recognition of template-primer and gapped DNA substrates by the human DNA polymerase β , *J. Mol. Biol.* 308, 477-500.
 22. Dominguez, O., Ruiz, J. F., de Lera, T. L., Garcia-Diaz, M., Gonzalez, M. A., Kirchhoff, T., Martinez, A., Bernad, A., and Blanco, L. (2000) DNA polymerase μ (Pol μ), homologous to TdT, could act as a DNA mutator in eukaryotic cells, *EMBO J.* 19, 1731-1742.
 23. Takahara, P. M., Rosenzweig, A. C., Frederick, C. A., and Lippard, S. J. (1995) Crystal structure of double-stranded DNA containing the major adduct of the anticancer drug cisplatin, *Nature* 377, 649-652.
 24. Gelasco, A., and Lippard, S. J. (1998) NMR solution structure of a DNA dodecamer duplex

containing a cis-diammineplatinum(II) dGpG intrastrand cross-link, the major adduct of the anticancer drug cisplatin, *Biochemistry* 37, 9230-9239.

25. Spingler, B., Whittington, D. A., and Lippard, S. J. (2001) 2.4 A crystal structure of an oxaliplatin 1,2-d(GpG) intrastrand cross-link in a DNA dodecamer duplex, *Inorg. Chem.* 40, 5596-5602.
26. Bassett, E., Vaisman, A., Tropea, K. A., McCall, C. M., Masutani, C., Hanaoka, F., and Chaney, S. G. (2002) Frameshifts and deletions during *in vitro* translesion synthesis past Pt-DNA adducts by DNA polymerases β and η , *DNA Repair* *In press*.
27. Mis, J. R. A., and Kunz, B. A. (1990) Analysis of mutations induced in the SUP4-o gene of *Saccharomyces cerevisiae* by cis-diammine dichloroplatinum(II), *Carcinogenesis* 11, 633-638.
28. de Boer, J. G., and Glickman, B. W. (1989) Sequence specificity of mutations induced by the antitumor drug cisplatin in the CHO *aprt* gene, *Carcinogenesis* 10, 1363-1367.
29. de Boer, J. G., and Glickman, B. W. (1992) Mutations Recovered in the Chinese Hamster *aprt* Gene After Exposure to Carboplatin - A Comparison with Cisplatin, *Carcinogenesis* 13, 15-17.

Figure 1: Structures and sequences of oligonucleotide templates with a single platinum adduct in a CTAGGC sequence context (the location of the platinum adduct is underlined) and a primer terminating immediately prior to the adduct. These primer-templates were used in primer extension and nucleotide incorporation assays. Primed single-stranded (A), 1 nt gap (B), 2 nt gap (C), 3 nt gap (D), and 4 nt gap (E). The site-specifically platinated oligonucleotides were constructed and hybridized to the primers (and acceptors) as described in Materials and Methods.

Figure 2: Primer extension with a primer terminating immediately prior to the adduct on CTAGGC templates of varying gap size. Representative gels showing primer extension experiments conducted with primed single-stranded templates for 0, 5, 15, 30, 45, 60, 120, and 180 m on undamaged templates (lanes 1-8), CP-damaged templates (lanes 9-16), and OX-damaged templates (lanes 17-24) (A); 1 nt gap templates for 0, 5, 10, and 15 m on undamaged templates (lanes 1-4), CP-damaged templates (lanes 5-8), and OX-damaged templates (lanes 9-12) (B); 2 nt gap templates for 0, 5, 10, 20, and 30 m on undamaged templates (lanes 1-5), CP-damaged templates (lanes 6-10), and OX-damaged templates (lanes 11-15) (C); 3 nt gap templates for 0, 10, 20, 30, and 45 m on undamaged templates (lanes 1-5), CP-damaged templates (lanes 6-10), and OX-damaged templates (lanes 11-15) (D); and 4 nt gap templates for 0, 10, 20, 30, and 45 m on undamaged templates (lanes 1-5), CP-damaged templates (lanes 6-10), and OX-damaged templates (lanes 11-15) (E). The template sequence of interest is indicated.

Figure 3: Effect of gap size on the ability of pol μ to catalyze chain elongation with a primer terminating immediately prior to the adduct on undamaged (A) and CP-damaged (B) CTAGGC templates. The graphs show a time course of chain elongation as a percentage of primer-termini elongated with primed single-stranded (\diamond), 1 nt gap (\circ), 2 nt gap (Δ), 3 nt gap (\square), and 4 nt gap (∇). Data are means (\pm standard error) from three to six independent experiments performed as described in Figure 2 and Materials and Methods. Where no error bars are seen the standard error was less than the

size of the symbol.

Figure 4: Effect of gap size on the ability of pol μ to catalyze chain elongation with a primer terminating immediately prior to the adduct on CTAGGC templates. Graphs show a time course of chain elongation on undamaged templates (\square) and translesion synthesis past CP (\circ) and OX (Δ) adducts on primed single-stranded templates (A), 1 nt (B), 2 nt (C), 3 nt (D), and 4 nt gapped templates (E). Data are means (\pm standard error) from three to six independent experiments. Where no error bars are seen the standard error was less than the size of the symbol.

Figure 5: Patterns of nucleotide incorporation with a primer terminating immediately prior to the adduct on CTAGGC templates. Representative gels show the specificity of nucleotide incorporation on various templates. Nucleotide incorporation studies were performed with individual dNTPs present at 500 μ M concentration (A, incubation with 500 μ M dATP; C, incubation with 500 μ M dCTP; G, incubation with 500 μ M dGTP; and T, incubation with 500 μ M dTTP). Incubations were performed with primed single-stranded templates for 30 m (A), 1 nt gapped templates for 5 m (B), 2 nt gapped templates for 20 m (C), 3 nt gapped templates for 20 m (D), and 4 nt gapped templates for 10 m (E). The template sequence of interest is indicated.

Figure 6: Relative frequency of nucleotide misincorporation with a primer terminating immediately prior to the adduct on CTAGGC templates. Graphs show the relative amount of dNTP misincorporation as compared to correct dCTP incorporation with undamaged (black bars), CP-damaged (light gray bars), and OX-damaged (dark gray bars) templates for dTTP misincorporation (A), dATP misincorporation (B), and dGTP misincorporation (C) on primed single-stranded templates (represented on graph as 0 nt gap size) and templates with 1, 2, 3, and 4 nt gaps. Data for graphical representation were obtained by dividing the mean of dNTP misincorporation by the mean of correct dCTP incorporation from two

experiments and the standard deviation was obtained using a standard proportional error formula.

Figure 7: Extent of chain elongation and pattern of nucleotide incorporation with a primer terminating immediately prior to the adduct on TCTGGT templates. The primer-templates used in these experiments with a 3 nt gap (A) and a 4 nt gap (B) are shown. The time course of chain elongation on undamaged templates (\square) and translesion synthesis past CP (\circ) and OX (\triangle) adducts on templates with a 3 nt gap (C) and on templates with a 4 nt gap (D). Data are means (\pm standard error) from three to six experiments. Where no error bars are seen the standard error was less than the size of the symbol. Pattern of nucleotide incorporation with undamaged (black bars), CP-damaged (light gray bars), and OX-damaged (dark gray bars) templates with 3 nt gap (E) and 4 nt gap (F). Data for graphical representation were obtained by dividing the mean of dNTP misincorporation by the mean of correct dCTP incorporation from two experiments and the standard deviation was obtained using a standard proportional error formula.

Figure 8: Structures and sequences of oligonucleotide templates with a single platinum adduct in a CTAGGC sequence context (the location of the platinum adduct is underlined) and a primer terminating across from the 3'G of the adduct. These primer-templates were used in primer extension and nucleotide incorporation assays. Primed single-stranded (A), 1 nt gap (B), 2 nt gap (C), and 3 nt gap (D) templates are shown. The site-specifically platinated oligonucleotides were constructed and hybridized to the primers (and acceptors) as described in Materials and Methods.

Figure 9: Primer extension with a primer terminating across from the 3'G of the adduct on CTAGGC templates of varying gap size. Representative gels showing primer extension experiments conducted with primed single-stranded templates for 0, 5, 10, 15, and 30 m on undamaged templates (lanes 1-5), CP-damaged templates (lanes 6-10), and OX-damaged templates (lanes 11-15) (A); 1 nt gap for 0, 5, 10,

20, and 30 m on undamaged templates (lanes 1-5), CP-damaged templates (lanes 6-10), and OX-damaged templates (lanes 11-15) (B); 2 nt gap for 0, 5, 10, 20, and 30 m on undamaged templates (lanes 1-5), CP-damaged templates (lanes 6-10), and OX-damaged templates (lanes 11-15) (C); and 3 nt gap for 0, 5, 10, 20, and 30 m on undamaged templates (lanes 1-5), CP-damaged templates (lanes 6-10), and OX-damaged templates (lanes 11-15) (D). The template sequence of interest is indicated.

Figure 10: Effect of gap size on the ability of pol μ to catalyze chain elongation with a primer terminating across from the 3'G of the adduct on CTAGGC templates. Graphs show a time course of chain elongation on undamaged templates (\square) and translesion synthesis past CP (\circ) and OX (\triangle) adducts on templates with primed single-stranded (A), 1 nt gap (B), 2 nt gap (C), and 3 nt gap (D) templates. Data are means (\pm standard error) from three experiments. Where no error bars are seen the standard error was less than the size of the symbol.

Figure 11: Relative frequency of nucleotide misincorporation with a primer terminating across from the 3'G of the adduct on CTAGGC templates. Graphs show the relative amount of dNTP misincorporation as compared to correct dCTP incorporation with undamaged (black bars), CP-damaged (light gray bars), and OX-damaged (dark gray bars) templates for dTTP misincorporation (A), dATP misincorporation (B), and dGTP misincorporation (C) on primed single-stranded templates (represented on graph as 0 nt gap size) and templates with 1, 2, and 3 nt gaps. Data for graphical representation were obtained by dividing the mean of dNTP misincorporation by the mean of correct dCTP incorporation from two experiments and the standard deviation was obtained using a standard proportional error formula.

Figure 1

A

5' *CACCATGCATCCTTCAATAGAAGG
3' GTGGTACGTAGGAAGTTATCTTCCGGATCTGCGGGTGGTGGTGG 5'

B

5' *CACCATGCATCCTTCAATAGAAGG CTAGACGCCCACCACCACC 3'
3' GTGGTACGTAGGAAGTTATCTTCCGGATCTGCGGGTGGTGGTGG 5'

C

5' *CACCATGCATCCTTCAATAGAAGG TAGACGCCCACCACCACC 3'
3' GTGGTACGTAGGAAGTTATCTTCCGGATCTGCGGGTGGTGGTGG 5'

D

5' *CACCATGCATCCTTCAATAGAAGG AGACGCCCACCACCACC 3'
3' GTGGTACGTAGGAAGTTATCTTCCGGATCTGCGGGTGGTGGTGG 5'

E

5' *CACCATGCATCCTTCAATAGAAGG GACGCCCACCACCACC 3'
3' GTGGTACGTAGGAAGTTATCTTCCGGATCTGCGGGTGGTGGTGG 5'

Figure 2

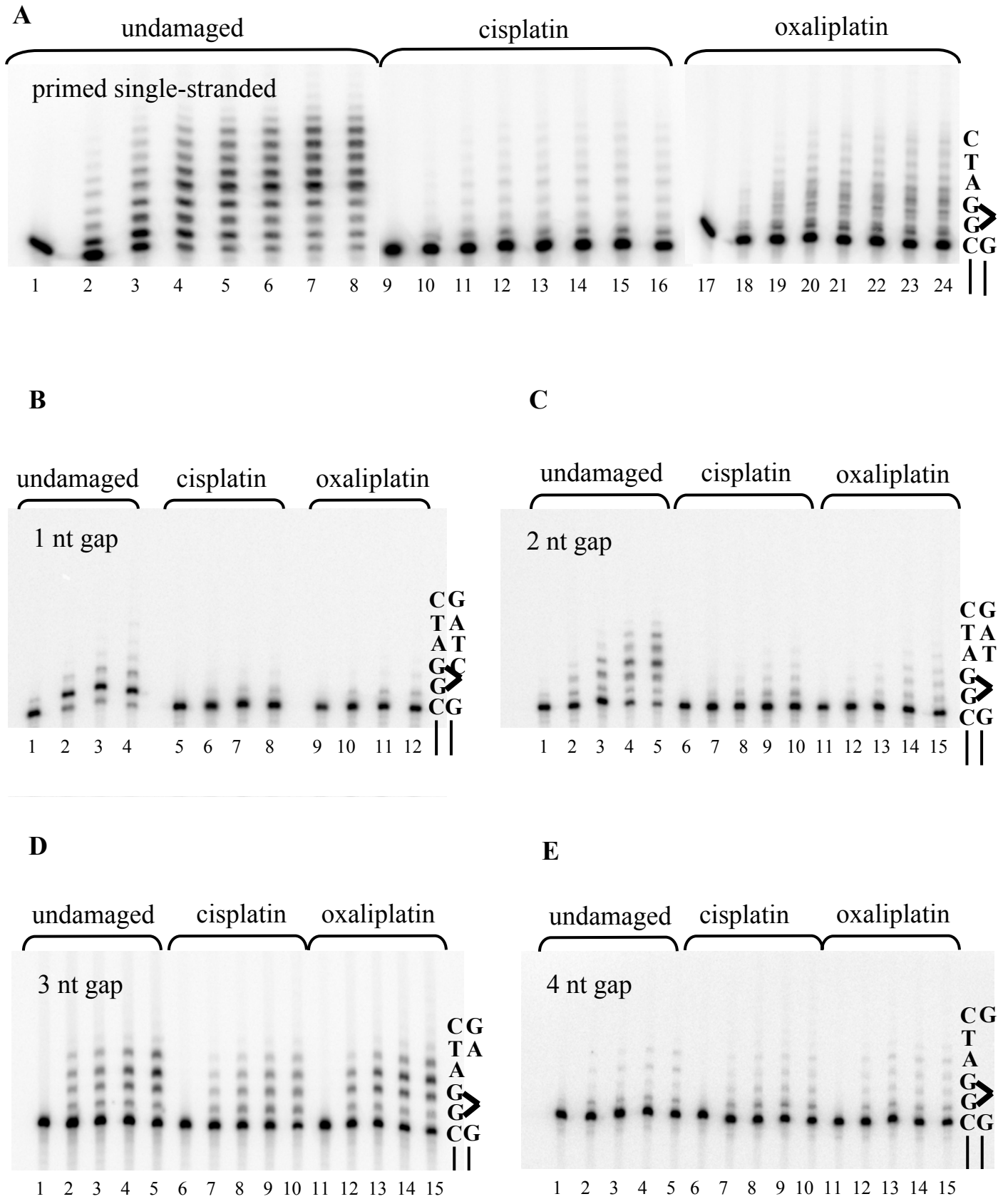


Figure 3

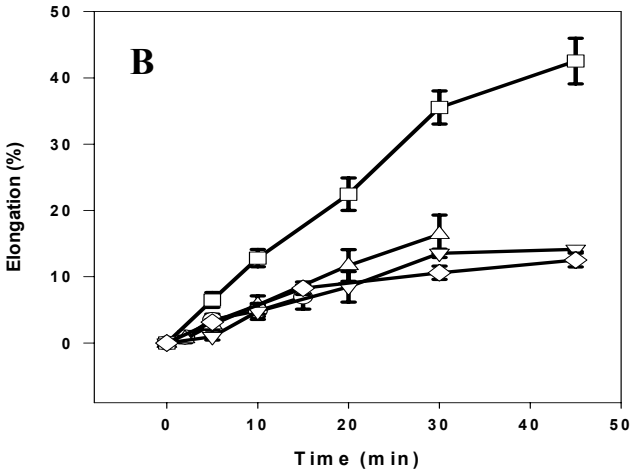
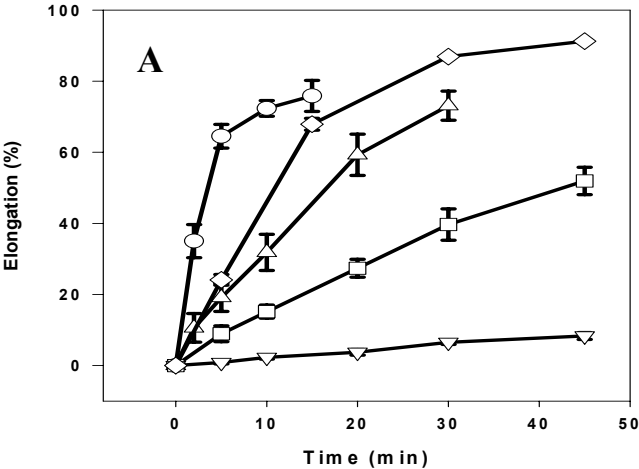


Figure 4

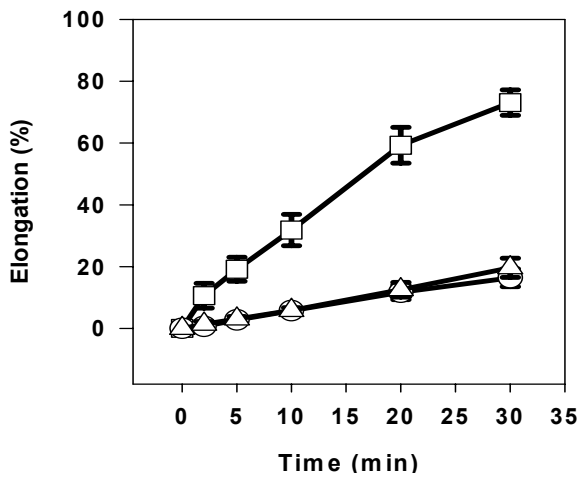
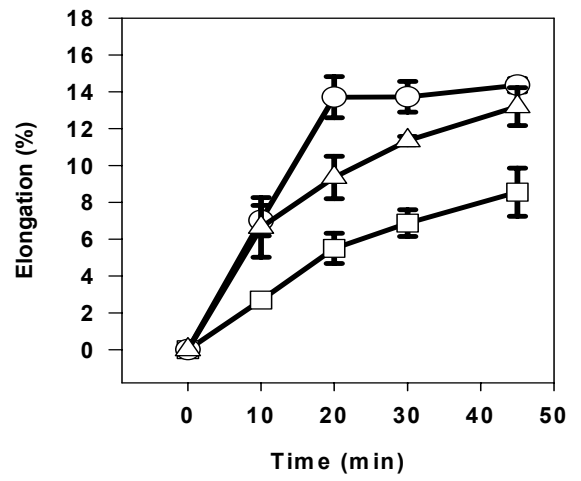
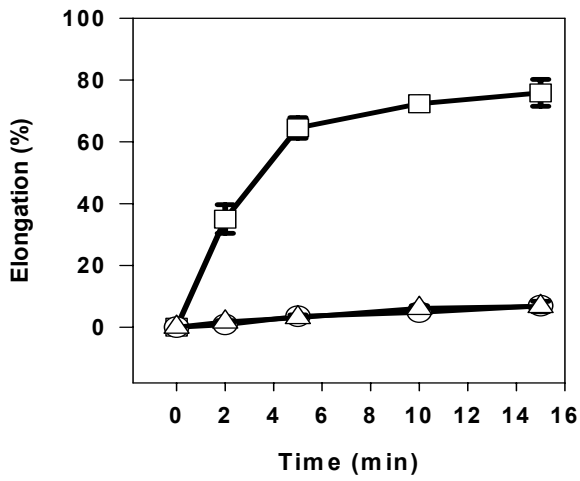
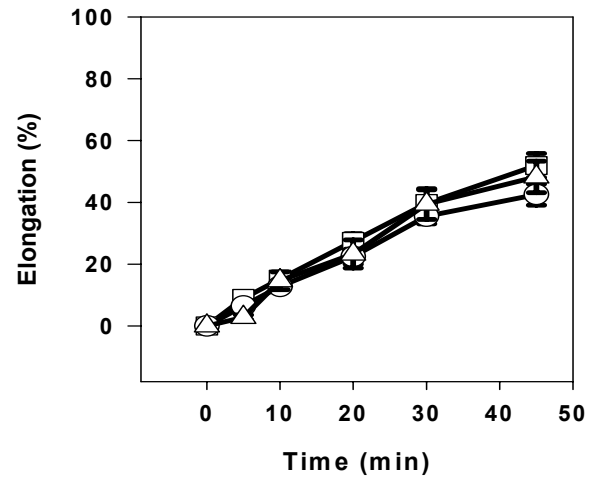
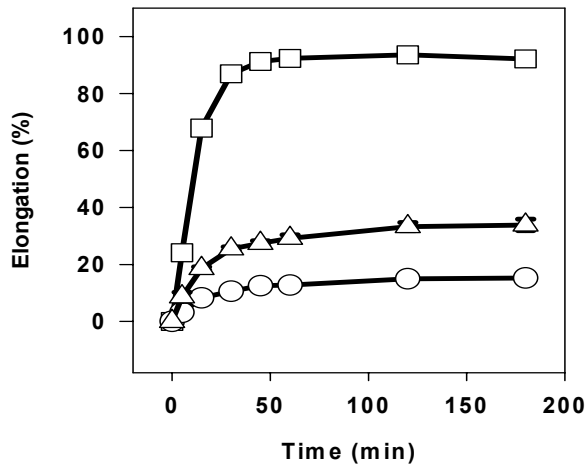


Figure 5

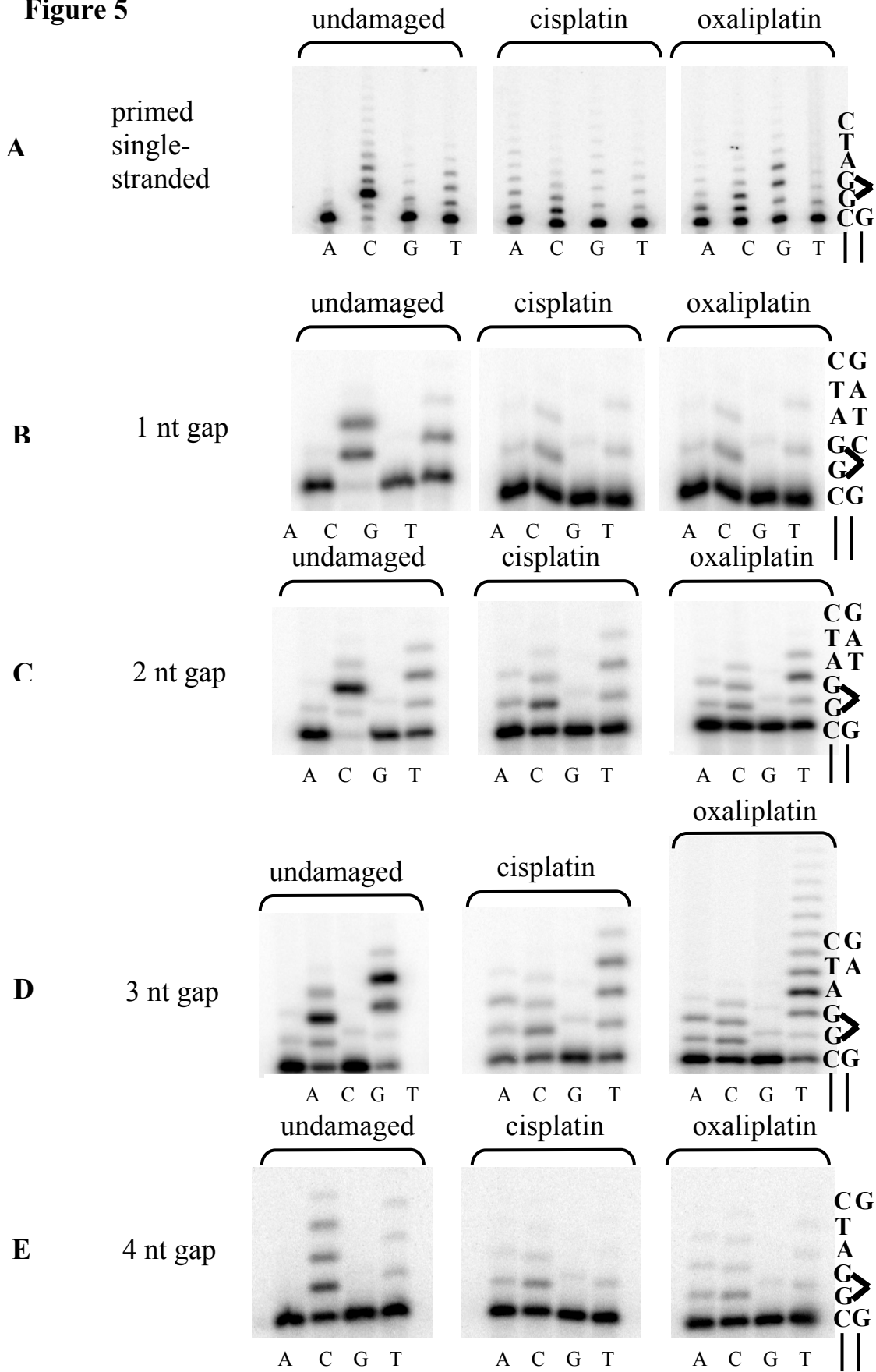


Figure 6

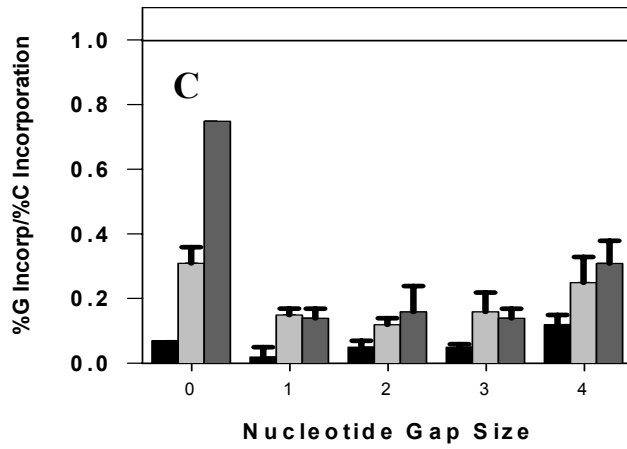
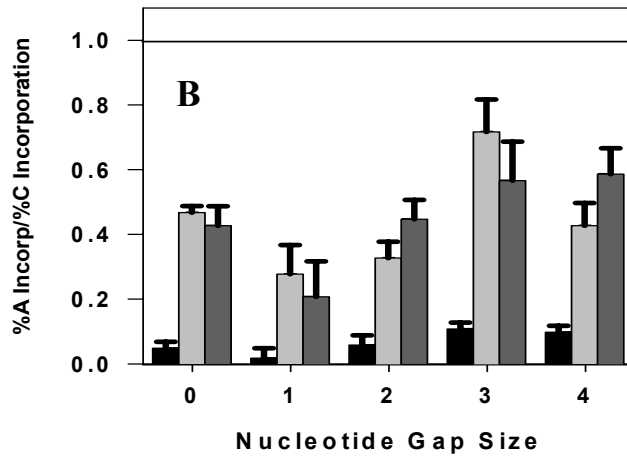
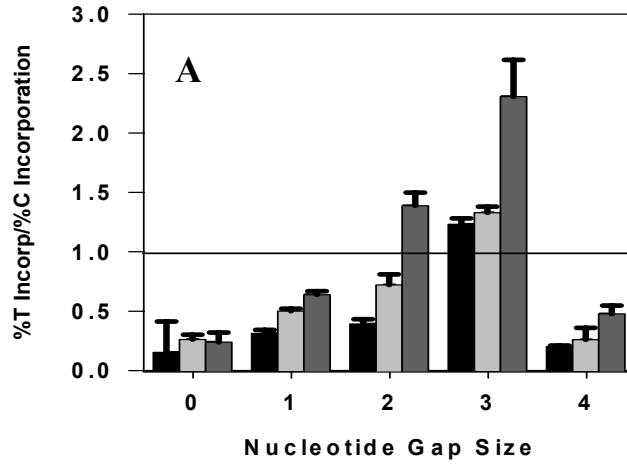


Figure 7

A

5' *GCATCCGGCAATCGAATTTAAAGA GAGCCGAACTCAGATCTACCACCACC 3'
 3' CGTAGGCCGTTAGCTTAAATTTCTGGTCTCGGGCTTGAGTCTAGATGGTGGTGG 5'

B

5' *GCATCCGGCAATCGAATTTAAAGA AGCCGAACTCAGATCTACCACCACC 3'
 3' CGTAGGCCGTTAGCTTAAATTTCTGGTCTCGGGCTTGAGTCTAGATGGTGGTGG 5'

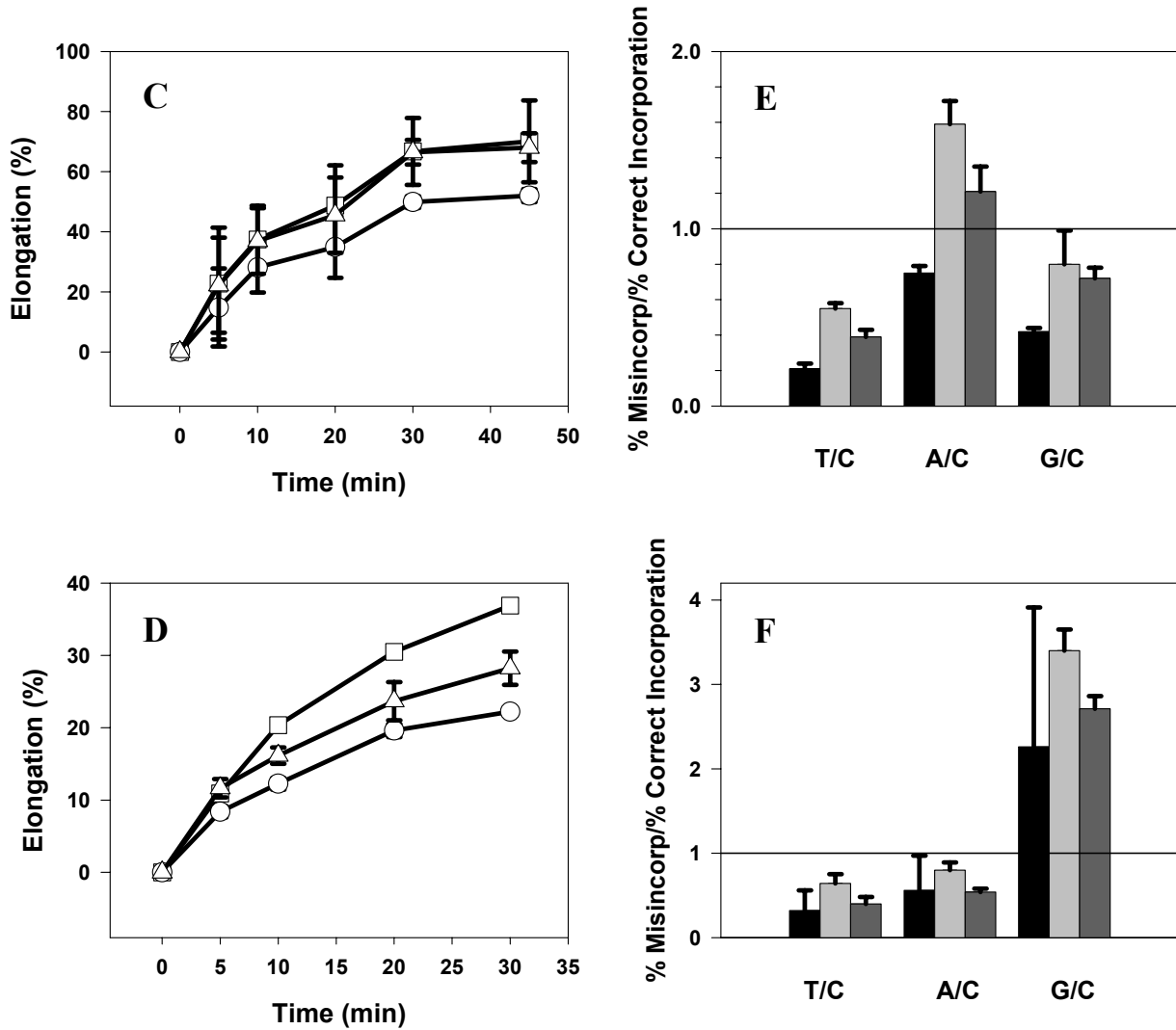


Figure 8

A

5' *CACCATGCATCCTTCAATAGAAGGC 3'
3' GTGGTACGTAGGAAGTTATCTTCCGGATCTGCGGGTGGTGGTGG 5'

B

5' *CACCATGCATCCTTCAATAGAAGGC TAGACGCCACCACCACC 3'
3' GTGGTACGTAGGAAGTTATCTTCCGGATCTGCGGGTGGTGGTGG 5'

C

5' *CACCATGCATCCTTCAATAGAAGGC AGACGCCACCACCACC 3'
3' GTGGTACGTAGGAAGTTATCTTCCGGATCTGCGGGTGGTGGTGG 5'

D

5' *CACCATGCATCCTTCAATAGAAGGC GACGCCACCACCACC 3'
3' GTGGTACGTAGGAAGTTATCTTCCGGATCTGCGGGTGGTGGTGG 5'

Figure 9

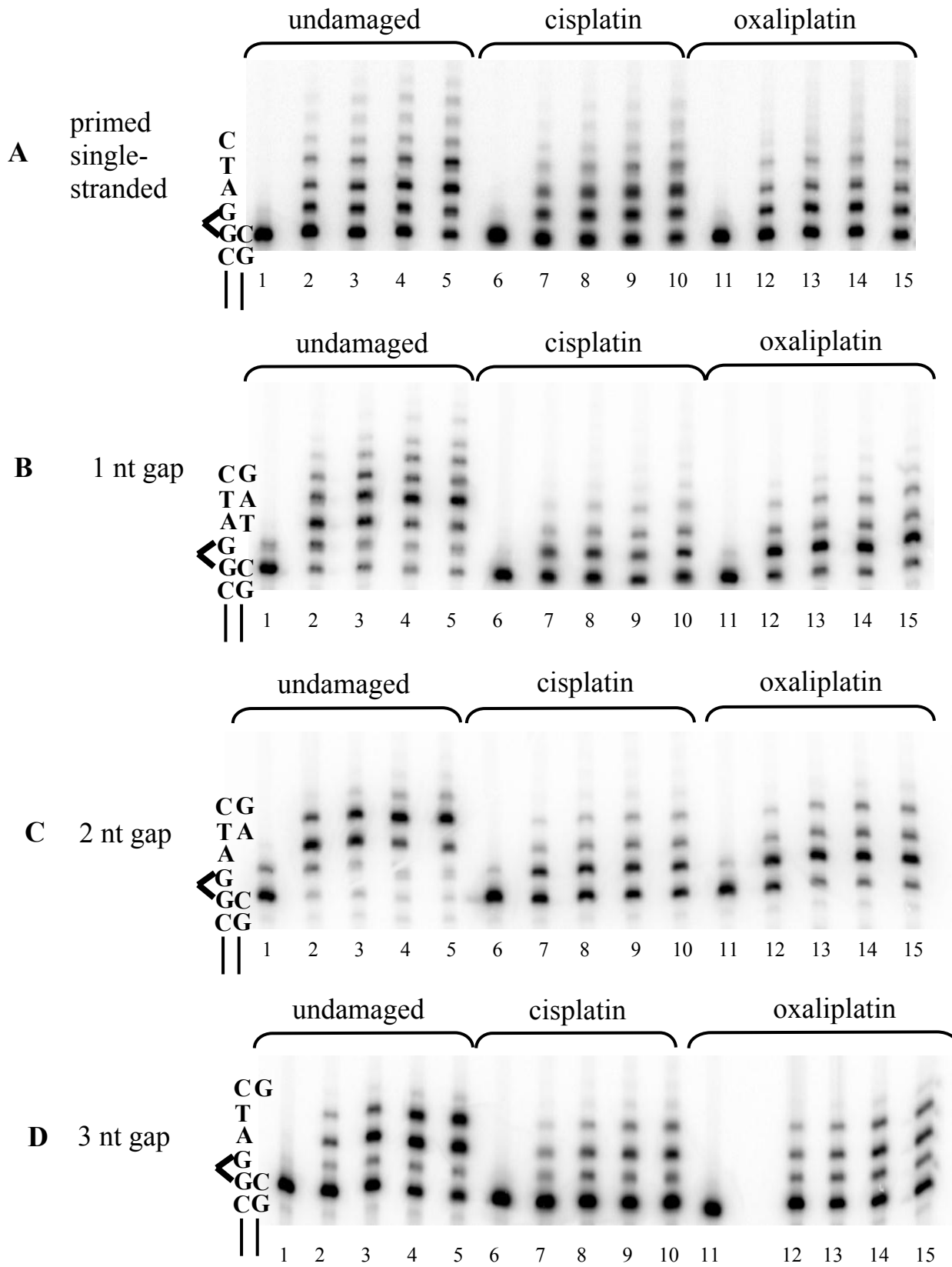


Figure 10

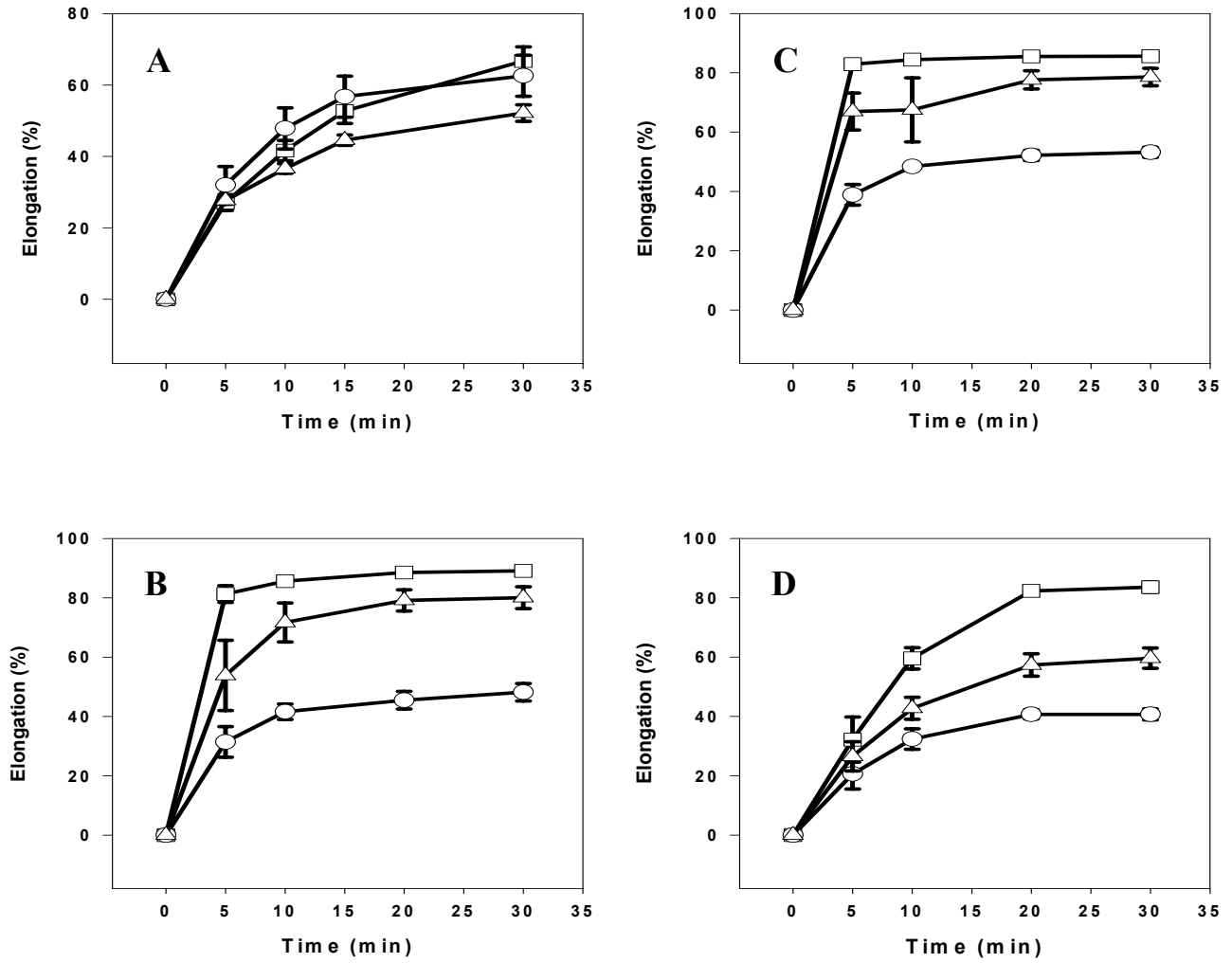


Figure 11

